

Cite as: B. Smith *et al.*, *Science* 10.1126/science.aaz5845 (2020).

Pervasive ice sheet mass loss reflects competing ocean and atmosphere processes

Ben Smith^{1*}, Helen A. Fricker², Alex S. Gardner³, Brooke Medley⁴, Johan Nilsson³, Fernando S. Paolo³, Nicholas Holschuh^{5,6}, Susheel Adusumilli², Kelly Brunt⁷, Bea Csathó⁸, Kaitlin Harbeck⁹, Thorsten Markus⁴, Thomas Neumann⁴, Matthew R. Siegfried¹⁰, H. Jay Zwally^{4,7}

¹University of Washington, Applied Physics Laboratory, Polar Science Center, Seattle, WA, USA. ²Scripps Institution of Oceanography, University of California, San Diego, CA, USA. ³Jet Propulsion Laboratory, California Institute of Technology, Pasadena, CA, USA. ⁴Cryospheric Science Lab, NASA Goddard Space Flight Center, Greenbelt, MD, USA. ⁵Department of Earth and Space Sciences, University of Washington, Seattle, WA, USA. ⁶Department of Geology, Amherst College, Amherst, MA, USA. ⁷Earth System Science Interdisciplinary Center, University of Maryland, College Park, MD, USA. ⁸Department of Geological Sciences, University at Buffalo, Buffalo, NY, USA. ⁹KBR, Greenbelt, MD, USA. ¹⁰Department of Geophysics, Colorado School of Mines, Golden, CO, USA.

*Corresponding author. Email: besmith@uw.edu

Quantifying changes in Earth's ice sheets, and identifying the climate drivers, is central to improving sea-level projections. We provide unified estimates of grounded and floating ice mass change from 2003 to 2019 using NASA's ICESat and ICESat-2 satellite laser altimetry. Our data reveal patterns likely linked to competing climate processes: Ice loss from coastal Greenland (increased surface melt), Antarctic ice shelves (increased ocean melting), and Greenland and Antarctic outlet glaciers (dynamic response to ocean melting), was partially compensated by mass gains over ice sheet interiors (increased snow accumulation). Losses outpaced gains, with grounded-ice loss from Greenland (200 Gt a^{-1}) and Antarctica (118 Gt a^{-1}) contributing 14 mm to sea level. Mass lost from West Antarctica's ice shelves accounted for over 30% of that region's total.

Observations of ice sheet mass change are essential to our understanding of present and future sea-level change (1–3). Ice sheets gain mass through snow accumulation and lose it through three processes: surface melt runoff (Greenland, 50–65%); iceberg calving (Antarctica ~50% and Greenland 15–25%); and basal melting of floating ice shelves (Antarctica, ~50%) and tidewater glaciers (Greenland, 15–25%) (4–6). The net balance between these competing processes largely dictates decadal to centennial ice-sheet contributions to sea level and depends on interactions between ice, ocean, and atmosphere. Surface meltwater runoff, basal melting, and precipitation are all expected to increase in a warming climate, which has been observed for both ice sheets (7, 8). In Greenland, with a sea-level potential of ~7 m, enhanced surface melt has resulted in widespread thinning of the ablation zone (9), and thinning and retreat of tidewater glacier fronts have led to accelerated flow (10), increased discharge toward the ocean (6), and near-coastal thinning (11–13) due to increased flux divergence. In Antarctica, with a sea-level potential of ~58 m, changes in ocean heat content linked to changes in Southern Hemisphere atmospheric conditions (14) have enhanced basal melting of ice shelves, causing them to shrink (15, 16), reducing their buttressing capability and leading to increased ice discharge into the ocean (17–20). Despite rapid advancement in our ability to observe the ice sheet response to climate change, it has been challenging to observe ice-mass changes associated with atmospheric and ocean forcing of

the ice sheets with a self-consistent data set. Here, we use measurements from NASA's Ice, Cloud and land Elevation Satellite (ICESat; 2003–2009) and ICESat-2 (2018–2019) to resolve precise patterns of ice sheet height change, which when combined with a new firn model provide a combined estimate of total grounded and floating mass change from both ice sheets. Although loss of floating ice makes no direct contribution to sea-level, it directly affects the rate of ice flow into the ocean. Patterns of change in floating and grounded ice together reveal the spatial signatures of the atmospheric and ocean processes that lead to grounded ice loss.

Satellite radar and laser altimeters have collected near continuous measurements since the early 1990s, providing one of the longest records of ice sheet change and revealing broad patterns of mass change across both ice sheets [e.g., (21, 22)]. In Antarctica, grounded ice changes have been qualitatively linked to floating ice shelf changes, but altimeter studies have all considered grounded ice [e.g., (1, 23)] and floating ice [e.g., (1, 16)] separately. The resulting differences in instruments, methodologies, and study periods can obscure connections between processes in grounded and floating ice, so a unified estimate of, for example, the ratio between grounded and floating ice loss has not been straightforward. Compared to radar altimetry, laser altimetry has the advantage of definitive measurement to the ice-sheet surface with minimal subsurface penetration, and the capability for accurate measurements over the steeper sloping ice-sheet

margins. ICESat, Earth's first polar-orbiting satellite laser altimeter, sampled the surface with small (~ 60 m) footprints and finer sampling (172 m), but results from that mission alone suffer from the short (six year) duration of the mission. Subtle changes in the ice sheet interiors have been difficult to capture due to measurement uncertainties [time-varying biases in radar altimetry (2) and ICESat (24)]. When integrated over the vast ice sheet area, these biases can overwhelm small, but significant, changes in ice-sheet mass balance from either trends in precipitation or long-term imbalance between ice flow and precipitation (1).

NASA's next generation laser altimeter ICESat-2 was designed to eliminate many of these problems. Launched 15 September 2018, ICESat-2 has a high sampling rate (0.7 m along-track), narrow footprint (~ 14.5 m), and near-global coverage ($\pm 88^\circ$ latitude) repeating every three months, with a six-beam geometry that enables instantaneous cross-track slope determination (fig. S1). We compare ICESat-2 data (October 2018 to February 2019) to data from the ICESat mission (September 2003 to October 2008), which sampled a more coarsely spaced set of tracks to $\pm 86^\circ$ latitude (Fig. 1A) (25). Elevation-change estimates from these instruments cover all of Greenland and 95% percent of Antarctica. We remove the influence of local topography between missions by extracting height-difference measurements only for locations where the two sets of tracks cross (Fig. 1, C and D). Because both measurements come from laser altimeters, they are not strongly biased due to subsurface scattering and retain their accuracy in sloping coastal regions. After aggregating the difference measurements into a regular grid, we estimate elevation-change rates and apply several corrections to obtain equivalent changes in mass, including a customized firn correction, state-of-the-art glacial isostatic adjustment, elastic compensation of the Earth's surface, ocean tides, and inverse barometer effect (25). We restrict our ice-shelf analysis to areas that were covered by ice shelves throughout both missions, so the ice-shelf mass changes directly associated with changes in ice-shelf extent are excluded from our estimates.

In Greenland, we find strong thinning that extends around the entire coastline (Fig. 2), which decreases inland, giving way to thickening at elevations between 2000 and 2500 m in western and southern Greenland and at elevations closer to 1500 m in the northeast. The largest thinning rates were between 4 and 6 m a^{-1} in Jakobshavn and Kangerdlugs-suaq glaciers, whereas the largest inland thickening rates were less than 0.15 m a^{-1} . The total mass change rate for the ice sheet between 2003 and 2019 was -200 ± 12 Gt a^{-1} , with a basin-by-basin variation from -48 ± 4 Gt a^{-1} in the Northwest to 2 ± 2 Gt a^{-1} in the Northeast (table S2). The low-elevation thinning is associated with both atmospheric and ocean processes: An increase in surface melt due to a combination of increases in both air temperatures and exposure of bare ice

during the summer [e.g., (26–28)]. At the same time, the combination of increased surface melt and warmer ocean temperatures has led to enhanced submarine melting of submerged glacier termini (29, 30) and has allowed more rapid calving by reducing the presence of rigid mélange in the fjords (31), each of which have increased glacier velocities and ice discharge into the ocean. With the exception of the Northeast, every sector of the ice sheet lost substantial mass during our period of investigation.

Some of the highest Greenland ice mass losses are in the northwest and southeast sectors, where strong dynamic changes took place shortly after the start of the ICESat mission (32). The recent acceleration in ice loss from Northeast Greenland (33) appears more limited in extent and magnitude and has less impact on the total mass balance. Despite the record-setting discharge rates of Jakobshavn Isbrae (34), its contribution is only around 10% of the Greenland mass loss between 2003 and 2019, in part because the rapid mass loss due to its acceleration in the late 1990s (35) declined with the slowing and thickening of the lower part of the glacier between 2013 and 2018 (36). Overall, loss of solid ice around the margins outpaces lower rates of snow gain distributed across the interior.

In Antarctica, we see broad scale patterns that are the fingerprints of two competing climate processes (snow accumulation and ocean melting) occurring on different spatial and temporal scales (Fig. 3), with strong connections between changes in grounded and floating ice in West Antarctica and the Antarctic Peninsula. The “background” pattern is one of subtle thickening along the steep slopes of the Antarctic Peninsula and around the coast to Queen Maud Land, East Antarctica, where gains decrease with distance from the ocean, indicative of snow accumulation in excess of that needed to balance flux divergence due to ice flow. This is likely due to enhanced moisture flux from marine air masses, but our measurements only provide an upper bound on the duration over which this may have occurred. Superimposed on this is a pattern of dramatic, ongoing mass loss around the margins, especially in the Amundsen and Bellingshausen regions of West Antarctica, likely in response to rapidly shrinking ice shelves. Ice shelf thinning in the Amundsen Sea has been attributed to an increase in atmospheric-driven incursions of modified Circumpolar Deep Water under the ice shelves, enhancing ocean-induced melting of marine-based basins (14, 16). Similar patterns may be emerging for marine-based outlet glaciers of East Antarctica, such as at Denman Glacier (Fig. 3), where a deep subglacial canyon and a retrograde slope may drive unstable retreat (37). The three large cold-water ice shelves (Ross, Filchner-Ronne and Amery) have smaller height-change rates, but there are striking internally driven changes where the stagnant Kamb Ice Stream (38) and slowing Whillans Ice Stream (39) starve downstream Ross Ice

Shelf of mass input (see fig. S8 for locations). In contrast to West Antarctic ice shelves, East Antarctic ice shelves gained $106 \pm 29 \text{ Gt a}^{-1}$ (Table 1).

The most significant floating-ice losses occurred along the Amundsen-Bellingshausen region of West Antarctica and the Antarctic peninsula. A basin-by-basin comparison between floating and grounded ice loss allows us to quantify the link between rapidly thinning ice shelves and grounded-ice loss in these regions: e.g., 53% of mass loss from the Getz Ice Shelf basin (basin 20) was from ice shelf mass loss, 29% for the Thwaites basin (basin 21), and 61% for the George VI Ice Shelf basin (basin 24). in West Antarctica. Overall, 31% of West Antarctic ice loss for 2003 to 2019 ($76 \pm 49 \text{ Gt a}^{-1}$) was from the ice shelves while the remaining 69% ($169 \pm 10 \text{ Gt a}^{-1}$) was from the grounded ice feeding those ice shelves (Table 1 and table S1); for the Antarctic Peninsula, 27% of the mass loss was from floating ice.

Considering only grounded ice (for sea-level contribution) our data show pervasive mass loss around the margins of Greenland, West Antarctica, and the Antarctic Peninsula, partially offset by mass gains in East Antarctica and central Greenland. Our mass loss rates of $118 \pm 24 \text{ Gt a}^{-1}$ from Antarctica and $200 \pm 12 \text{ Gt a}^{-1}$ from Greenland imply a total sea-level contribution of $14 \pm 1 \text{ mm}$ over the 16-year period (Table 1). Compared with a compilation of mass-change estimates for a similar time span (2002–2017) (2), our Antarctic estimates are consistent (within reported errors) for the Antarctic Peninsula and for the whole ice sheet, but significantly more positive for East Antarctica ($90 \pm 21 \text{ vs. } 2 \pm 37 \text{ Gt a}^{-1}$) and significantly more negative for West Antarctica ($-169 \pm 10 \text{ vs. } -124 \pm 27 \text{ Gt a}^{-1}$). For Greenland, our estimate is consistent with rates derived from a compilation of techniques that extends through 2018 (40), but is significantly more positive than some rates calculated from mass-flux techniques between 2003 and 2018 ($-200 \pm 21 \text{ vs. } -268 \pm 14 \text{ Gt a}^{-1}$) (41). Another recent mass-flux-based estimate (42) gives modestly larger loss rates for Greenland ($-233 \pm 12 \text{ Gt a}^{-1}$), with differences that arise in part because that estimate includes mass changes in peripheral ice and tundra that our study excludes. Because our height-change estimates have smaller instrumental biases than previous laser-altimetry estimates, our results strongly suggest that earlier disagreement between some input-output and altimetry estimates (1, 8) was at least partially due to negative biases in the input-output estimates. Despite this, our results show that the mass gains in East Antarctica are not sufficient to offset the rapid mass losses from West Antarctica and the Antarctic Peninsula, so that Antarctica's contribution to sea level change is unambiguously positive.

We estimated height changes for both ice sheets (grounded and floating ice) from NASA's ICESat and ICESat-2 laser altimetry missions (2003 to 2019). Applying novel

corrections to convert from height to mass change, we generated maps of mass changes for the ice sheets. Our maps highlight complex localized patterns of ocean-induced changes near the coast where inland ice is responding to increased frontal melt and ice shelf thinning by flowing faster, leading to increased flux divergence and surface lowering, with the strongest signals visible in the Amundsen and Bellingshausen coasts of Antarctica. Mixed signals, including the effects of surface melting and ocean-driven velocity changes, are apparent around the coasts of Greenland. We also see more subtle thickening across the vast interiors of the ice sheets, likely in response increased snowfall, where the precision of height-change measurements by previous altimeters limited inferences of mass change. For both ice sheets, these patterns result from the interplay between the ocean and atmosphere; ultimately, high elevation gains are greatly outmatched by low elevation dynamic losses, combined with enhanced surface melting in Greenland.

Our unified estimates of grounded and floating ice sheet mass change show that overall, Greenland lost $200 \pm 12 \text{ Gt a}^{-1}$, while Antarctica lost a total of 103 Gt a^{-1} , with $118 \pm 24 \text{ Gt a}^{-1}$ from grounded ice and a small net gain of $15 \pm 65 \text{ Gt a}^{-1}$ from ice shelves. Together, the ice sheets contributed $\sim 14 \text{ mm}$ sea level equivalent to the world's oceans over that 16-year period (8.9 mm from Greenland and 5.2 mm from Antarctica). In West Antarctica, ice loss from ice shelves (which does not directly contribute to sea level change) accounted for 31% of the total mass loss, and all West Antarctic marine basins with ice grounded below sea level (which are sensitive to flow instabilities, and whose losses directly contribute to sea-level change) are out of balance. Given the susceptibility of ice shelves and floating glacier termini to changing atmospheric and oceanic conditions, and of grounded ice to shrinking ice shelves (43), we can expect increasing contribution from both Greenland and Antarctica to sea level rise on relatively short (decadal to centennial) time scales.

REFERENCES AND NOTES

1. A. Shepherd, E. R. Ivins, G. A. V. R. Barletta, M. J. Bentley, S. Bettadpur, K. H. Briggs, D. H. Bromwich, R. Forsberg, N. Galin, M. Horwath, S. Jacobs, I. Joughin, M. A. King, J. T. M. Lenaerts, J. Li, S. R. M. Ligtenberg, A. Luckman, S. B. Luthcke, M. McMillan, R. Meister, G. Milne, J. Mouginot, A. Muir, J. P. Nicolas, J. Paden, A. J. Payne, H. Pritchard, E. Rignot, H. Rott, L. S. Sørensen, T. A. Scambos, B. Scheuchl, E. J. O. Schrama, B. Smith, A. V. Sundal, J. H. van Angelen, W. J. van de Berg, M. R. van den Broeke, D. G. Vaughan, I. Velicogna, J. Wahr, P. L. Whitehouse, D. J. Wingham, D. Yi, D. Young, H. J. Zwally, A reconciled estimate of ice-sheet mass balance. *Science* **338**, 1183–1189 (2012). doi:[10.1126/science.1228102](https://doi.org/10.1126/science.1228102) Medline
2. IMBIE team, Mass balance of the Antarctic Ice Sheet from 1992 to 2017. *Nature* **558**, 219–222 (2018). doi:[10.1038/s41586-018-0179-y](https://doi.org/10.1038/s41586-018-0179-y) Medline
3. J. L. Bamber, R. M. Westaway, B. Marzeion, B. Wouters, The land ice contribution to sea level during the satellite era. *Environ. Res. Lett.* **13**, 63008 (2018). doi:[10.1088/1748-9326/aac2f0](https://doi.org/10.1088/1748-9326/aac2f0)
4. D. I. Benn, T. Cowton, J. Todd, A. Luckman, Glacier Calving in Greenland. *Curr. Clim. Change Rep.* **3**, 282–290 (2017). doi:[10.1007/s40641-017-0070-1](https://doi.org/10.1007/s40641-017-0070-1) Medline
5. M. A. Depoorter, J. L. Bamber, J. A. Griggs, J. T. M. Lenaerts, S. R. M. Ligtenberg, M. R. van den Broeke, G. Moholdt, Calving fluxes and basal melt rates of Antarctic ice shelves. *Nature* **502**, 89–92 (2013). doi:[10.1038/nature12567](https://doi.org/10.1038/nature12567) Medline

6. E. Rignot, S. Jacobs, J. Mouginot, B. Scheuchl, Ice-shelf melting around Antarctica. *Science* **341**, 266–270 (2013). [doi:10.1126/science.1235798](https://doi.org/10.1126/science.1235798) Medline
7. J. T. M. Lenaerts, B. Medley, M. R. van den Broeke, B. Wouters, Observing and Modeling Ice Sheet Surface Mass Balance. *Rev. Geophys.* **57**, 376–420 (2019). [doi:10.1029/2018RG000622](https://doi.org/10.1029/2018RG000622) Medline
8. E. Rignot, J. Mouginot, B. Scheuchl, M. van den Broeke, M. J. van Wessem, M. Morlighem, Four decades of Antarctic Ice Sheet mass balance from 1979–2017. *Proc. Natl. Acad. Sci. U.S.A.* **116**, 1095–1103 (2019). [doi:10.1073/pnas.1812883116](https://doi.org/10.1073/pnas.1812883116) Medline
9. M. van den Broeke, J. Bamber, J. Ettema, E. Rignot, E. Schrama, W. J. van de Berg, E. van Meijgaard, I. Velicogna, B. Wouters, Partitioning recent Greenland mass loss. *Science* **326**, 984–986 (2009). [doi:10.1126/science.1178176](https://doi.org/10.1126/science.1178176) Medline
10. I. Joughin, B. E. Smith, I. M. Howat, D. Floricioiu, A. B. Richard, M. Truffer, M. Fahnestock, Seasonal to decadal scale variations in the surface velocity of Jakobshavn Isbrae, Greenland: Observation and model-based analysis. *J. Geophys. Res. Earth Surf.* **117**, (2012). [doi:10.1029/2011JF002110](https://doi.org/10.1029/2011JF002110)
11. B. M. Csatho, A. F. Schenck, C. J. van der Veen, G. Babonis, K. Duncan, S. Rezvanbehbahani, M. R. van den Broeke, S. B. Simonsen, S. Nagarajan, J. H. van Angelen, Laser altimetry reveals complex pattern of Greenland Ice Sheet dynamics. *Proc. Natl. Acad. Sci. U.S.A.* **111**, 18478–18483 (2014). [doi:10.1073/pnas.1411680112](https://doi.org/10.1073/pnas.1411680112) Medline
12. I. M. Howat, B. E. Smith, I. Joughin, T. A. Scambos, Rates of southeast Greenland ice volume loss from combined ICESat and ASTER observations. *Geophys. Res. Lett.* **35**, L17505 (2008). [doi:10.1029/2008GL034496](https://doi.org/10.1029/2008GL034496)
13. N. Wilson, F. Straneo, P. Heimbach, Satellite-derived submarine melt rates and mass balance (2011–2015) for Greenland’s largest remaining ice tongues. *Cryosphere* **11**, 2773–2782 (2017). [doi:10.5194/tc-11-2773-2017](https://doi.org/10.5194/tc-11-2773-2017)
14. M. Thoma, A. Jenkins, D. Holland, S. Jacobs, Modelling Circumpolar Deep Water intrusions on the Amundsen Sea continental shelf, Antarctica. *Geophys. Res. Lett.* **35**, L18602 (2008). [doi:10.1029/2008GL034939](https://doi.org/10.1029/2008GL034939)
15. H. D. Pritchard, S. R. M. Ligtenberg, H. A. Fricker, D. G. Vaughan, M. R. van den Broeke, L. Padman, Antarctic ice-sheet loss driven by basal melting of ice shelves. *Nature* **484**, 502–505 (2012). [doi:10.1038/nature10968](https://doi.org/10.1038/nature10968) Medline
16. F. S. Paolo, H. A. Fricker, L. Padman, Ice sheets. Volume loss from Antarctic ice shelves is accelerating. *Science* **348**, 327–331 (2015). [doi:10.1126/science.aaa0940](https://doi.org/10.1126/science.aaa0940) Medline
17. J. J. Fürst, G. Durand, F. Gillet-Chaulet, L. Tavard, M. Rankl, M. Braun, O. Gagliardini, The safety band of Antarctic ice shelves. *Nat. Clim. Chang.* **6**, 479–482 (2016). [doi:10.1038/nclimate2912](https://doi.org/10.1038/nclimate2912)
18. T. K. Dupont, R. B. B. Alley, Assessment of the importance of ice-shelf buttressing to ice-sheet flow. *Geophys. Res. Lett.* **32**, 1–4 (2005). [doi:10.1029/2004GL022024](https://doi.org/10.1029/2004GL022024)
19. T. A. Scambos, J. A. Bohlander, C. A. Shuman, P. Skvarca, Glacier acceleration and thinning after ice shelf collapse in the Larsen B embayment, Antarctica. *Geophys. Res. Lett.* **31**, L18402 (2004). [doi:10.1029/2004GL020670](https://doi.org/10.1029/2004GL020670)
20. E. Rignot, J. Mouginot, M. Morlighem, H. Seroussi, B. Scheuchl, Widespread, rapid grounding line retreat of Pine Island, Thwaites, Smith, and Kohler glaciers, West Antarctica, from 1992 to 2011. *Geophys. Res. Lett.* **41**, 3502–3509 (2014). [doi:10.1002/2014GL060140](https://doi.org/10.1002/2014GL060140)
21. D. J. Wingham, A. Shepherd, A. Muir, G. J. Marshall, Mass balance of the Antarctic ice sheet. *Philos. Trans. A Math. Phys. Eng. Sci.* **364**, 1627–1635 (2006). [doi:10.1098/rsta.2006.1792](https://doi.org/10.1098/rsta.2006.1792) Medline
22. H. J. Zwally, M. B. Giovinetto, J. Li, H. G. Cornejo, M. A. Beckley, A. C. Brenner, J. L. Saba, D. Yi, Mass changes of the Greenland and Antarctic ice sheets and shelves and contributions to sea-level rise: 1992–2002. *J. Glaciol.* **51**, 509–527 (2005). [doi:10.3189/172756505781829007](https://doi.org/10.3189/172756505781829007)
23. H. D. Pritchard, R. J. Arthern, D. G. Vaughan, L. A. Edwards, Extensive dynamic thinning on the margins of the Greenland and Antarctic ice sheets. *Nature* **461**, 971–975 (2009). [doi:10.1038/nature08471](https://doi.org/10.1038/nature08471) Medline
24. A. A. Borsa, H. A. Fricker, K. M. Brunt, A Terrestrial Validation of ICESat Elevation Measurements and Implications for Global Reanalyses. *IEEE Trans. Geosci. Remote Sens.* **57**, 6946–6959 (2019). [doi:10.1109/TGRS.2019.2909739](https://doi.org/10.1109/TGRS.2019.2909739)
25. Materials and methods are available as supplementary materials at the Science website.
26. J. C. Ryan, A. Hubbard, M. Stibal, T. D. Irvine-Fynn, J. Cook, L. C. Smith, K. Cameron, J. Box, Dark zone of the Greenland Ice Sheet controlled by distributed biologically-active impurities. *Nat. Commun.* **9**, 1065 (2018). [doi:10.1038/s41467-018-03353-2](https://doi.org/10.1038/s41467-018-03353-2) Medline
27. M. R. van den Broeke, E. M. Enderlin, I. M. Howat, P. Kuipers Munneke, B. P. Y. Noël, W. J. van de Berg, E. van Meijgaard, B. Wouters, On the recent contribution of the Greenland ice sheet to sea level change. *Cryosphere* **10**, 1933–1946 (2016). [doi:10.5194/tc-10-1933-2016](https://doi.org/10.5194/tc-10-1933-2016)
28. X. Fettweis, J. E. Box, C. Agosta, C. Amory, C. Kittel, C. Lang, D. Van As, H. Machguth, H. Gallée, Reconstructions of the 1900–2015 Greenland ice sheet surface mass balance using the regional climate MAR model. *Cryosphere* **11**, 1015–1033 (2017). [doi:10.5194/tc-11-1015-2017](https://doi.org/10.5194/tc-11-1015-2017)
29. M. Wood, E. Rignot, I. Fenty, D. Menemenlis, R. Millan, M. Morlighem, J. Mouginot, H. Seroussi, Ocean-Induced Melt Triggers Glacier Retreat in Northwest Greenland. *Geophys. Res. Lett.* **45**, 8334–8342 (2018). [doi:10.1029/2018GL078024](https://doi.org/10.1029/2018GL078024)
30. D. Slater, F. Straneo, D. Felikson, C. Little, H. Goelzer, X. Fettweis, J. Holte, Estimating Greenland tidewater glacier retreat driven by submarine melting. *Cryosphere* **13**, 2489–2509 (2019). [doi:10.5194/tc-13-2489-2019](https://doi.org/10.5194/tc-13-2489-2019)
31. T. Moon, I. Joughin, B. Smith, Seasonal to multiyear variability of glacier surface velocity, terminus position, and sea ice/ice mélange in northwest Greenland. *J. Geophys. Res. Earth Surf.* **120**, 818–833 (2015). [doi:10.1002/2015JF003494](https://doi.org/10.1002/2015JF003494)
32. E. Rignot, P. Kanagaratnam, Changes in the velocity structure of the Greenland Ice Sheet. *Science* **311**, 986–990 (2006). [doi:10.1126/science.1121381](https://doi.org/10.1126/science.1121381) Medline
33. S. A. Khan, K. H. Kjær, M. Bevis, J. L. Bamber, J. Wahr, K. K. Kjeldsen, A. B. Bjørk, N. J. Korsgaard, L. A. Stearns, M. R. van den Broeke, L. Liu, N. K. Larsen, I. S. Muresan, Sustained mass loss of the northeast Greenland ice sheet triggered by regional warming. *Nat. Clim. Chang.* **4**, 292–299 (2014). [doi:10.1038/nclimate2161](https://doi.org/10.1038/nclimate2161)
34. I. Joughin, B. E. Smith, D. E. Shean, D. Floricioiu, Brief Communication: Further summer speedup of Jakobshavn Isbrae. *Cryosphere* **8**, 209–214 (2014). [doi:10.5194/tc-8-209-2014](https://doi.org/10.5194/tc-8-209-2014)
35. I. Joughin, W. Abdalati, M. Fahnestock, Large fluctuations in speed on Greenland’s Jakobshavn Isbrae glacier. *Nature* **432**, 608–610 (2004). [doi:10.1038/nature03130](https://doi.org/10.1038/nature03130) Medline
36. A. Khazendar, I. G. Fenty, D. Carroll, A. Gardner, C. M. Lee, I. Fukumori, O. Wang, H. Zhang, H. Seroussi, D. Moller, B. P. Y. Noël, M. R. van den Broeke, S. Dinardo, J. Willis, Interruption of two decades of Jakobshavn Isbrae acceleration and thinning as regional ocean cools. *Nat. Geosci.* **12**, 277–283 (2019). [doi:10.1038/s41561-019-0329-3](https://doi.org/10.1038/s41561-019-0329-3)
37. M. Morlighem, E. Rignot, T. Binder, D. Blankenship, R. Drews, G. Eagles, O. Eisen, F. Ferraccioli, R. Forsberg, P. Fretwell, V. Goel, J. S. Greenbaum, H. Gudmundsson, J. Guo, V. Helm, C. Hofstede, I. Howat, A. Humbert, W. Jokat, N. B. Karlsson, W. S. Lee, K. Matsuoka, R. Millan, J. Mouginot, J. Paden, F. Pattyn, J. Roberts, S. Rosier, A. Ruppel, H. Seroussi, E. C. Smith, D. Steinhage, B. Sun, M. R. van den Broeke, T. D. van Ommen, M. van Wessem, D. A. Young, Deep glacial troughs and stabilizing ridges unveiled beneath the margins of the Antarctic ice sheet. *Nat. Geosci.* **13**, 132–137 (2020). [doi:10.1038/s41561-019-0510-8](https://doi.org/10.1038/s41561-019-0510-8)
38. G. A. Catania, T. A. Scambos, H. Conway, C. F. Raymond, Sequential stagnation of Kamb Ice Stream, West Antarctica. *Geophys. Res. Lett.* **33**, L14502 (2006). [doi:10.1029/2006GL026430](https://doi.org/10.1029/2006GL026430)
39. L. H. Beem, S. M. Tulaczyk, M. A. King, M. Bougamont, H. A. Fricker, P. Christoffersen, Variable deceleration of Whillans Ice Stream, West Antarctica. *J. Geophys. Res. Earth Surf.* **119**, 212–224 (2014). [doi:10.1002/2013JF002958](https://doi.org/10.1002/2013JF002958)
40. IMBIE Team, Mass balance of the Greenland Ice Sheet from 1992 to 2018. *Nature* **579**, 233–239 (2020). [doi:10.1038/s41586-019-1855-2](https://doi.org/10.1038/s41586-019-1855-2) Medline
41. J. Mouginot, E. Rignot, A. B. Bjørk, M. van den Broeke, R. Millan, M. Morlighem, B. Noël, B. Scheuchl, M. Wood, Forty-six years of Greenland Ice Sheet mass balance from 1972 to 2018. *Proc. Natl. Acad. Sci. U.S.A.* **116**, 9239–9244 (2019). [doi:10.1073/pnas.1904242116](https://doi.org/10.1073/pnas.1904242116) Medline
42. M. D. King, I. M. Howat, S. Jeong, M. J. Noh, B. Wouters, B. Noël, M. R. van den Broeke, Seasonal to decadal variability in ice discharge from the Greenland Ice Sheet. *Cryosphere* **12**, 3813–3825 (2018). [doi:10.5194/tc-12-3813-2018](https://doi.org/10.5194/tc-12-3813-2018) Medline

43. G. H. Gudmundsson, F. S. Paolo, S. Adusumilli, H. A. Fricker, Instantaneous Antarctic ice sheet mass loss driven by thinning ice shelves. *Geophys. Res. Lett.* **46**, 13903–13909 (2019). [doi:10.1029/2019GL085027](https://doi.org/10.1029/2019GL085027)
44. K. J. Tinto, L. Padman, C. S. Siddoway, S. R. Springer, H. A. Fricker, I. Das, F. Caratori Tontini, D. F. Porter, N. P. Frearson, S. L. Howard, M. R. Siegfried, C. Mosbeux, M. K. Becker, C. Bertinato, A. Boghosian, N. Brady, B. L. Burton, W. Chu, S. I. Cordero, T. Dhakal, L. Dong, C. D. Gustafson, S. Keeshin, C. Locke, A. Lockett, G. O'Brien, J. J. Spergel, S. E. Starke, M. Tankersley, M. G. Wearing, R. E. Bell, Ross Ice Shelf response to climate driven by the tectonic imprint on seafloor bathymetry. *Nat. Geosci.* **12**, 441–449 (2019). [doi:10.1038/s41561-019-0370-2](https://doi.org/10.1038/s41561-019-0370-2)
45. X. Sun, J. B. Abshore, A. A. Borsa, H. A. Fricker, D. Yi, J. P. DiMarzio, F. S. Paolo, K. M. Brunt, D. J. Harding, G. A. Neumann, ICESat/GLAS Altimetry Measurements: Received Signal Dynamic Range and Saturation Correction. *IEEE Trans. Geosci. Remote Sens.* **55**, 5440–5454 (2017). [doi:10.1109/TGRS.2017.2702126](https://doi.org/10.1109/TGRS.2017.2702126) Medline
46. B. E. Schutz, H. J. Zwally, C. A. Shuman, D. Hancock, J. P. DiMarzio, Overview of the ICESat mission. *Geophys. Res. Lett.* **32**, L21S01 (2005). [doi:10.1029/2005GL024009](https://doi.org/10.1029/2005GL024009)
47. J. B. Abshore, X. Sun, H. Riris, J. M. Sirota, J. F. McGarry, S. Palm, D. Yi, P. Liiva, Geoscience Laser Altimeter System (GLAS) on the ICESat mission: On-orbit measurement performance. *Geophys. Res. Lett.* **32**, L21S02 (2005). [doi:10.1029/2005GL024028](https://doi.org/10.1029/2005GL024028)
48. T. Markus, T. Neumann, A. Martino, W. Abdalati, K. Brunt, B. Csatho, S. Farrell, H. Fricker, A. Gardner, D. Harding, M. Jasinski, R. Kwok, L. Magruder, D. Lubin, S. Luthcke, J. Morison, R. Nelson, A. Neuenschwander, S. Palm, S. Popescu, C. K. Shum, B. E. Schutz, B. Smith, Y. Yang, J. Zwally, The Ice, Cloud, and Land Elevation Satellite-2 (ICESat-2): Science requirements, concept, and implementation. *Remote Sens. Environ.* **190**, 260–273 (2017). [doi:10.1016/j.rse.2016.12.029](https://doi.org/10.1016/j.rse.2016.12.029)
49. D. Felikson, T. C. Bartholomaus, G. A. Catania, N. J. Korsgaard, K. H. Kjær, M. Morlighem, B. Noël, M. van den Broeke, L. A. Stearns, E. L. Shroyer, D. A. Sutherland, J. D. Nash, Inland thinning on the Greenland ice sheet controlled by outlet glacier geometry. *Nat. Geosci.* **10**, 366–369 (2017). [doi:10.1038/ngeo2934](https://doi.org/10.1038/ngeo2934)
50. T. A. Neumann, A. J. Martino, T. Markus, S. Bae, M. R. Bock, A. C. Brenner, K. M. Brunt, J. Cavanaugh, S. T. Fernandes, D. W. Hancock, K. Harbeck, J. Lee, N. T. Kurtz, P. J. Luers, S. B. Luthcke, L. Magruder, T. A. Pennington, L. Ramos-Izquierdo, T. Rebold, J. Skoog, T. C. Thomas, The Ice, Cloud, and Land Elevation Satellite-2 Mission: A global geolocated photon product derived from the advanced topographic laser altimeter system. *Remote Sens. Environ.* **233**, 111325 (2019). [doi:10.1016/j.rse.2019.111325](https://doi.org/10.1016/j.rse.2019.111325) Medline
51. B. Smith, H. A. Fricker, N. Holschuh, A. S. Gardner, S. Adusumilli, K. M. Brunt, B. Csatho, K. Harbeck, A. Huth, T. Neumann, J. Nilsson, M. R. Siegfried, Land ice height-retrieval algorithm for NASA's ICESat-2 photon-counting laser altimeter. *Remote Sens. Environ.* **233**, 111352 (2019). [doi:10.1016/j.rse.2019.111352](https://doi.org/10.1016/j.rse.2019.111352)
52. R. Kwok, G. F. Cunningham, J. Hoffmann, T. Markus, Testing the ice-water discrimination and freeboard retrieval algorithms for the ICESat-2 mission. *Remote Sens. Environ.* **183**, 13–25 (2016). [doi:10.1016/j.rse.2016.05.011](https://doi.org/10.1016/j.rse.2016.05.011)
53. A. Neuenschwander, K. Pitts, The ATL08 land and vegetation product for the ICESat-2 Mission. *Remote Sens. Environ.* **221**, 247–259 (2019). [doi:10.1016/j.rse.2018.11.005](https://doi.org/10.1016/j.rse.2018.11.005)
54. S. C. Popescu, T. Zhou, R. Nelson, A. Neuenschwander, R. Sheridan, L. Narine, K. M. Walsh, Photon counting LiDAR: An adaptive ground and canopy height retrieval algorithm for ICESat-2 data. *Remote Sens. Environ.* **208**, 154–170 (2018). [doi:10.1016/j.rse.2018.02.019](https://doi.org/10.1016/j.rse.2018.02.019)
55. H. J. Zwally, R. Schutz, C. Bentley, J. Bufton, T. Herring, J. Minster, J. Spinhirne, R. Thomas, GLAS/ICESat L2 Antarctic and Greenland Ice Sheet Altimetry Data, version 34 (National Snow and Ice Data Center, 2014); [doi:10.5067/ICESAT/GLAS/DATA225](https://doi.org/10.5067/ICESAT/GLAS/DATA225)
56. A. A. Borsa, G. Moholdt, H. A. Fricker, K. M. Brunt, A range correction for ICESat and its potential impact on ice-sheet mass balance studies. *Cryosphere* **8**, 345–357 (2014). [doi:10.5194/tc-8-345-2014](https://doi.org/10.5194/tc-8-345-2014)
57. L. Padman, H. A. Fricker, R. Coleman, S. Howard, L. Erofeeva, A new tide model for the Antarctic ice shelves and seas. *Ann. Glaciol.* **34**, 247–254 (2002). [doi:10.3189/172756402781817752](https://doi.org/10.3189/172756402781817752)
58. G. D. Egbert, A. F. Bennett, M. G. G. Foreman, TOPEX/POSEIDON tides estimated using a global inverse model. *J. Geophys. Res. Atmos.* **99**, 821–852 (1994). [doi:10.1029/94JC01894](https://doi.org/10.1029/94JC01894)
59. G. D. Egbert, S. Y. Erofeeva, Efficient inverse modeling of barotropic ocean tides. *J. Atmos. Ocean. Technol.* **19**, 183–204 (2002). [doi:10.1175/1520-0426\(2002\)019<0183:EIMOB>2.0.CO;2](https://doi.org/10.1175/1520-0426(2002)019<0183:EIMOB>2.0.CO;2)
60. B. Smith, H. A. Fricker, A. Gardner, M. R. Siegfried, S. Adusumilli, B. M. Csathó, N. Holschuh, J. Nilsson, F. S. Paolo, The ICESat-2 Science Team, ATLAS/ICESat-2 L3A Land Ice Height, version 1 (National Snow and Ice Data Center, 2019); [doi:10.5067/ATLAS/ATL06.001](https://doi.org/10.5067/ATLAS/ATL06.001)
61. H. J. Zwally, J. Li, J. W. Robbins, J. L. Saba, D. Yi, A. C. Brenner, Mass gains of the Antarctic Ice Sheet exceed losses. *J. Glaciol.* **61**, 1019–1036 (2015). [doi:10.3189/2015JoG15J071](https://doi.org/10.3189/2015JoG15J071)
62. C. H. Davis, A. C. Ferguson, Elevation change of the Sntarctic Ice Sheet, 1995–2000, from ERS-2 satellite radar altimetry. *IEEE Trans. Geosci. Remote Sens.* **42**, 2437–2445 (2004). [doi:10.1109/TGRS.2004.836789](https://doi.org/10.1109/TGRS.2004.836789)
63. F. S. Paolo, H. A. Fricker, L. Padman, Constructing improved decadal records of Antarctic ice shelf height change from multiple satellite radar altimeters. *Remote Sens. Environ.* **177**, 192–205 (2016). [doi:10.1016/j.rse.2016.01.026](https://doi.org/10.1016/j.rse.2016.01.026)
64. S. R. M. Ligtenberg, M. M. Helsen, M. R. van den Broeke, An improved semi-empirical model for the densification of Antarctic firn. *Cryosphere* **5**, 809–819 (2011). [doi:10.5194/tc-5-809-2011](https://doi.org/10.5194/tc-5-809-2011)
65. P. Kuipers Munneke, S. R. M. Ligtenberg, B. P. Y. Noël, I. M. Howat, J. E. Box, E. Mosley-Thompson, J. R. McConnell, K. Steffen, J. T. Harper, S. B. Das, M. R. van den Broeke, Elevation change of the Greenland Ice Sheet due to surface mass balance and firn processes, 1960–2013. *Cryosphere Discuss.* **9**, 3541–3580 (2015). [doi:10.5194/tcd-9-3541-2015](https://doi.org/10.5194/tcd-9-3541-2015)
66. C. M. Stevens, thesis, University of Washington (2018).
67. J. M. D. Lundin, C. M. Stevens, R. Arthern, C. Buzert, A. Orsi, S. R. M. Ligtenberg, S. B. Simonsen, E. Cummings, R. Essery, W. Leahy, P. Harris, M. M. Helsen, E. D. Waddington, Firn Model Intercomparison Experiment (FirnMICE). *J. Glaciol.* **63**, 401–422 (2017). [doi:10.1017/jog.2016.114](https://doi.org/10.1017/jog.2016.114)
68. M. M. Herron, C. C. Langway, Firn Densification: An Empirical Model. *J. Glaciol.* **25**, 373–385 (1980). [doi:10.1017/S0022143000015239](https://doi.org/10.1017/S0022143000015239)
69. J. Li, H. J. Zwally, Modeling the density variation in the shallow firn layer. *Ann. Glaciol.* **38**, 309–313 (2004). [doi:10.3189/172756404781814988](https://doi.org/10.3189/172756404781814988)
70. J. Li, H. J. Zwally, Response times of ice-sheet surface heights to changes in the rate of Antarctic firn compaction caused by accumulation and temperature variations. *J. Glaciol.* **61**, 1037–1047 (2015). [doi:10.3189/2015JoG14J182](https://doi.org/10.3189/2015JoG14J182)
71. R. J. Arthern, D. G. Vaughan, A. M. Rankin, R. Mulvaney, E. R. Thomas, In situ measurements of Antarctic snow compaction compared with predictions of models. *J. Geophys. Res. Earth Surf.* **115**, 1–12 (2010).
72. V. Verjans, A. A. Leeson, C. M. Stevens, M. MacFerrin, B. Noël, M. R. van den Broeke, Development of physically based liquid water schemes for Greenland firn-densification models. *Cryosphere* **13**, 1819–1842 (2019). [doi:10.5194/tc-13-1819-2019](https://doi.org/10.5194/tc-13-1819-2019)
73. E. Rignot, J. Mouginot, B. Scheuchl, M. van den Broeke, M. J. van Wessem, M. Morlighem, Four decades of Antarctic Ice Sheet mass balance from 1979–2017. *Proc. Natl. Acad. Sci. U.S.A.* **116**, 1095–1103 (2019). [doi:10.1073/pnas.1812883116](https://doi.org/10.1073/pnas.1812883116) Medline
74. R. Gelaro, W. McCarty, M. J. Suárez, R. Todling, A. Molod, L. Takacs, C. Randles, A. Darmenov, M. G. Bosilovich, R. Reichle, K. Wargan, L. Coy, R. Cullather, C. Draper, S. Akella, V. Buchard, A. Conaty, A. da Silva, W. Gu, G. K. Kim, R. Koster, R. Lucchesi, D. Merkova, J. E. Nielsen, G. Partyka, S. Pawson, W. Putman, M. Riendecker, S. D. Schubert, M. Sienkiewicz, B. Zhao, The modern-era retrospective analysis for research and applications, version 2 (MERRA-2). *J. Clim.* **30**, 5419–5454 (2017). [doi:10.1175/JCLI-D-16-0758.1](https://doi.org/10.1175/JCLI-D-16-0758.1) Medline
75. B. Medley, E. R. Thomas, Increased snowfall over the Antarctic Ice Sheet mitigated twentieth-century sea-level rise. *Nat. Clim. Chang.* **9**, 34–39 (2019). [doi:10.1038/s41558-018-0356-x](https://doi.org/10.1038/s41558-018-0356-x)
76. B. Huai, Y. Wang, M. Ding, J. Zhang, X. Dong, An assessment of recent global atmospheric reanalyses for Antarctic near surface air temperature. *Atmos. Res.* **226**, 181–191 (2019). [doi:10.1016/j.atmosres.2019.04.029](https://doi.org/10.1016/j.atmosres.2019.04.029)
77. B. Noël, W. J. van de Berg, J. M. van Wessem, E. van Meijgaard, D. van As, J. T. M. Lenaerts, S. Lhermitte, P. Kuipers Munneke, C. J. P. P. Smeets, L. H. van Ulft, R. S. W. van de Wal, M. R. van den Broeke, Modelling the climate and surface mass balance of polar ice sheets using RACMO2 - Part 1: Greenland (1958–2016). *Cryosphere* **12**, 811–831 (2018). [doi:10.5194/tc-12-811-2018](https://doi.org/10.5194/tc-12-811-2018)

78. J. M. van Wessem, W. J. van de Berg, B. P. Y. Noël, E. van Meijgaard, C. Amory, G. Birnbaum, C. L. Jakobs, K. Krüger, J. T. M. Lenaerts, S. Lhermitte, S. R. M. Ligtenberg, B. Medley, C. H. Reijmer, K. van Tricht, L. D. Trusel, L. H. van Uift, B. Wouters, J. Wuute, M. R. van den Broeke, Modelling the climate and surface mass balance of polar ice sheets using RACMO2, part 2: Antarctica (1979–2016). *Cryosphere* **12**, 1479–1498 (2018). doi:[10.5194/tc-12-1479-2018](https://doi.org/10.5194/tc-12-1479-2018)
79. C. Agosta, C. Amory, C. Kittel, A. Orsi, V. Favier, H. Gallée, M. R. van den Broeke, J. T. M. Lenaerts, J. M. van Wessem, X. Fettweis, Estimation of the Antarctic surface mass balance using MAR (1979–2015) and identification of dominant processes. *Cryosphere Discuss.* **13**, 1–22 (2018).
80. M. van den Broeke, C. Bus, J. Ettema, P. Smeets, Temperature thresholds for degree-day modelling of Greenland ice sheet melt rates. *Geophys. Res. Lett.* **37**, 1–5 (2010). doi:[10.1029/2010GL044123](https://doi.org/10.1029/2010GL044123)
81. L. D. Trusel, K. E. Frey, S. B. Das, P. K. Munneke, M. R. van den Broeke, Satellite-based estimates of Antarctic surface meltwater fluxes. *Geophys. Res. Lett.* **40**, 6148–6153 (2013). doi:[10.1002/2013GL058138](https://doi.org/10.1002/2013GL058138)
82. H. Zwally, Jay, Mario B. Giovinetto, Matthew A. Beckley, and Jack L. Saba, 2012, Antarctic and Greenland Drainage Systems, GSFC Cryospheric Sciences Laboratory, at http://icesat4.gsfc.nasa.gov/cryo_data/ant_grn_drainage_systems.php.
83. S. R. M. Ligtenberg, M. M. Helsen, M. R. van den Broeke, An improved semi-empirical model for the densification of Antarctic firn. *Cryosphere* **5**, 809–819 (2011). doi:[10.5194/tc-5-809-2011](https://doi.org/10.5194/tc-5-809-2011)
84. P. Kuipers Munneke, S. R. M. Ligtenberg, B. P. Y. Noël, I. M. Howat, J. E. Box, E. Mosley-Thompson, J. R. McConnell, K. Steffen, J. T. Harper, S. B. Das, M. R. van den Broeke, Elevation change of the Greenland Ice Sheet due to surface mass balance and firn processes, 1960–2014. *Cryosphere* **9**, 2009–2025 (2015). doi:[10.5194/tc-9-2009-2015](https://doi.org/10.5194/tc-9-2009-2015)
85. A. S. Gardner, G. Moholdt, T. Scambos, M. Fahnestock, S. Ligtenberg, M. van den Broeke, J. Nilsson, Increased West Antarctic and unchanged East Antarctic ice discharge over the last 7 years. *Cryosphere* **12**, 521–547 (2018). doi:[10.5194/tc-12-521-2018](https://doi.org/10.5194/tc-12-521-2018)
86. J. Fyke, J. T. M. Lenaerts, H. Wang, Basin-scale heterogeneity in Antarctic precipitation and its impact on surface mass variability. *Cryosphere* **11**, 2595–2609 (2017). doi:[10.5194/tc-11-2595-2017](https://doi.org/10.5194/tc-11-2595-2017)
87. E. R. Ivins, T. S. James, J. Wahr, E. J. O. Schrama, F. W. Landerer, K. M. Simon, Antarctic contribution to sea level rise observed by GRACE with improved GIA correction. *J. Geophys. Res. Solid Earth* **118**, 3126–3141 (2013). doi:[10.1002/grb.50208](https://doi.org/10.1002/grb.50208)
88. P. L. Whitehouse, M. J. Bentley, G. A. Milne, M. A. King, I. D. Thomas, A new glacial isostatic adjustment model for Antarctica: Calibrated and tested using observations of relative sea-level change and present-day uplift rates. *Geophys. J. Int.* **190**, 1464–1482 (2012). doi:[10.1111/j.1365-246X.2012.05557.x](https://doi.org/10.1111/j.1365-246X.2012.05557.x)
89. K. G. Miller, J. D. Wright, J. V. Browning, A. Kulpeck, M. Komintz, T. R. Naish, B. S. Cramer, Y. Rosenthal, W. R. Peltier, S. Sosdian, High tide of the warm pliocene: Implications of global sea level for Antarctic deglaciation. *Geology* **40**, 407–410 (2012). doi:[10.1130/G32869.1](https://doi.org/10.1130/G32869.1)
90. W. Richard Peltier, D. F. Argus, R. Drummond, Comment on “An Assessment of the ICE-6G_C (VM5a) Glacial Isostatic Adjustment Model” by Purcell et al. *J. Geophys. Res. Solid Earth* **123**, 2019–2028 (2018). doi:[10.1002/2016JB013844](https://doi.org/10.1002/2016JB013844)
91. M. J. R. Simpson, G. A. Milne, P. Huybrechts, A. J. Long, Calibrating a glaciological model of the Greenland ice sheet from the Last Glacial Maximum to present-day using field observations of relative sea level and ice extent. *Quat. Sci. Rev.* **28**, 1631–1657 (2009). doi:[10.1016/j.quascirev.2009.03.004](https://doi.org/10.1016/j.quascirev.2009.03.004)
92. J. Wahr, D. Wingham, C. Bentley, A method of combining ICESat and GRACE satellite data to constrain Antarctic mass balance. *J. Geophys. Res. Solid Earth* **105** (B7), 16279–16294 (2000). doi:[10.1029/2000JB900113](https://doi.org/10.1029/2000JB900113)
93. W. E. Farrell, Deformation of the Earth by surface loads. *Rev. Geophys.* **10**, 761–797 (1972). doi:[10.1029/RG010i003p00761](https://doi.org/10.1029/RG010i003p00761)
94. H. R. Martens, L. Rivera, M. Simons, LoadDef: A Python-Based Toolkit to Model Elastic Deformation Caused by Surface Mass Loading on Spherically Symmetric Bodies. *Earth Space Sci.* **6**, 311–323 (2019). doi:[10.1029/2018EA000462](https://doi.org/10.1029/2018EA000462) Medline
95. A. M. Dziewonski, D. L. Anderson, Preliminary reference Earth model. *Phys. Earth Planet. Inter.* **25**, 297–356 (1981). doi:[10.1016/0031-9201\(81\)90046-7](https://doi.org/10.1016/0031-9201(81)90046-7)
96. M. A. Lazzara, K. C. Jezek, T. A. Scambos, D. R. MacAyeal, C. J. Van Der Veen, On the recent calving of icebergs from the Ross ice shelf. *Polar Geogr.* **31**, 15–26 (1999). doi:[10.1080/10889370802175937](https://doi.org/10.1080/10889370802175937)
97. H. A. Fricker, N. W. Young, I. Allison, R. Coleman, Iceberg calving from the Amery Ice Shelf, East Antarctica. *Ann. Glaciol.* **34**, 241–246 (2002). doi:[10.3189/172756402781817581](https://doi.org/10.3189/172756402781817581)
98. J. Mouginot, B. Scheuchl, E. Rignot, MEaSUREs Antarctic Boundaries for IPY 2007–2009 from Satellite Radar, version 2, (National Snow and Ice Data Center, 2017); [10.5067/AXF4121732AD](https://doi.org/10.5067/AXF4121732AD)
99. A. E. Hogg, G. H. Gudmundsson, Impacts of the Larsen-C Ice Shelf calving event. *Nat. Clim. Chang.* **7**, 540–542 (2017). doi:[10.1038/nclimate3359](https://doi.org/10.1038/nclimate3359)
100. K. M. Brunt, T. A. Neumann, C. F. Larsen, Assessment of altimetry using ground-based GPS data from the 88S Traverse, Antarctica, in support of ICESat-2. *Cryosphere* **13**, 579–590 (2019). doi:[10.5194/tc-13-579-2019](https://doi.org/10.5194/tc-13-579-2019)
101. K. M. Brunt, T. A. Neumann, B. E. Smith, First assessment of ICESat-2 Ice-Sheet surface heights, based on comparisons over the interior of the Antarctic ice sheet. *Geophys. Res. Lett.* (2019). doi:<https://doi.org/10.1029/2019GL084886>
102. J. F. Zumberge, M. B. Heflin, D. C. Jefferson, M. M. Watkins, F. H. Webb, Precise point positioning for the efficient and robust analysis of GPS data from large networks. *J. Geophys. Res. Solid Earth* **102** (B3), 5005–5017 (1997). doi:[10.1029/96JB03860](https://doi.org/10.1029/96JB03860)

ACKNOWLEDGMENTS

We would like to thank the ICESat-2 project and the ICESat-2 science team for enormous contributions to this project. We are also grateful to two anonymous reviewers for their constructive and insightful reviews. **Funding:** This work was funded by NASA Cryospheric Sciences Program in support of the ICESat-2 mission under the following awards: NNX15AE15G (Smith); NNX15AC80G (Fricker); NNX16AM01G (Holschuh); NNX17AI03G (Fricker). Alex Gardner, Johan Nilsson, and Fernando Serrano Paolo's efforts were funded by the NASA Cryospheric Sciences and NASA MEaSUREs programs through direct award to Alex Gardner. **Author contributions:** Fricker, Smith, Gardner conceptualized the study and, with Paolo, wrote the majority of the main text. Medley conducted firn and climate modeling. Paolo, Adusumilli, and Nilsson performed altimetry data processing. Holschuh, Paolo, Nilsson, and Gardner developed figures. Brunt provided insights into error models and calibrations. Csatho, Siegfried, and Zwally provided insights into altimetry and data analysis. Neumann, Markus, and Harbeck were responsible for the success of the ICESat-2 mission. All authors contributed to the writing and editing of the manuscript. **Competing interests:** The authors report no competing interests. **Data availability:** ICESat data are available at <https://nsidc.org/data/gla12> and the ICESat-2 data are available at <https://nsidc.org/data/atl06>. Mass-change grids are available from <https://digital.lib.washington.edu/researchworks/handle/1773/45388> (accession number 45388).

SUPPLEMENTARY MATERIALS

science.sciencemag.org/cgi/content/full/science.aaz5845/DC1
Materials and Methods
Supplementary Text
Figs. S1 to S8
Tables S1 and S2
References (45–102)

20 September 2019; accepted 13 April 2020

Published online 30 April 2020

10.1126/science.aaz5845

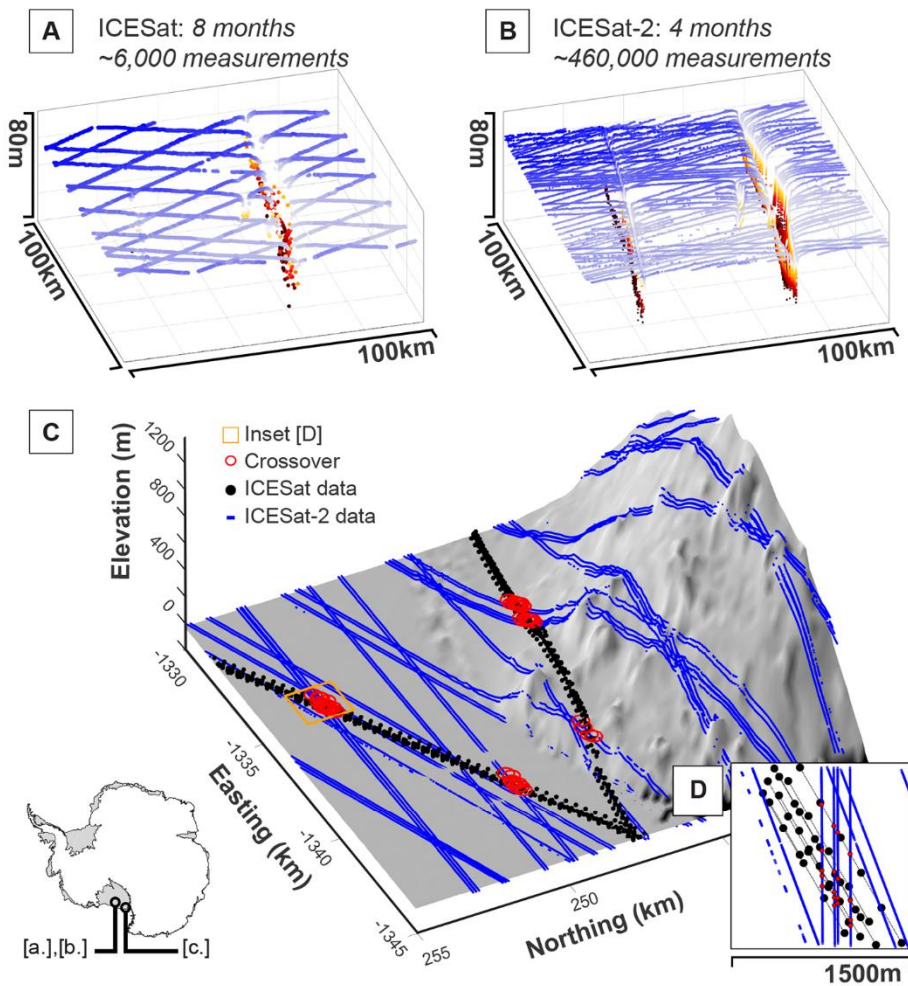


Fig. 1. Relative observation density of ICESat and ICESat-2 over the same target: rifts of Ross Ice Shelf. (A) ICESat. (B) ICESat-2. Increased along-track resolution and cross-track observation density allow us to capture high-slope, small-scale features in unprecedented detail. (C and D) ICESat–ICESat-2 surface height comparison is done at the survey crossover points (red). ICESat-2's small footprint and dense along-track spacing [(D), to scale], combined with its repeat-track mission design, will result in the most precise measurements of height-change rates available to date.

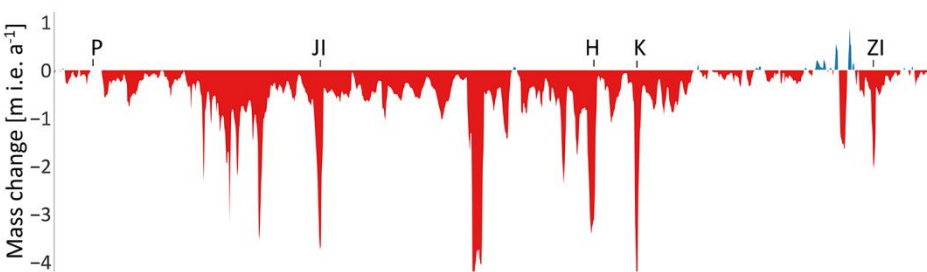
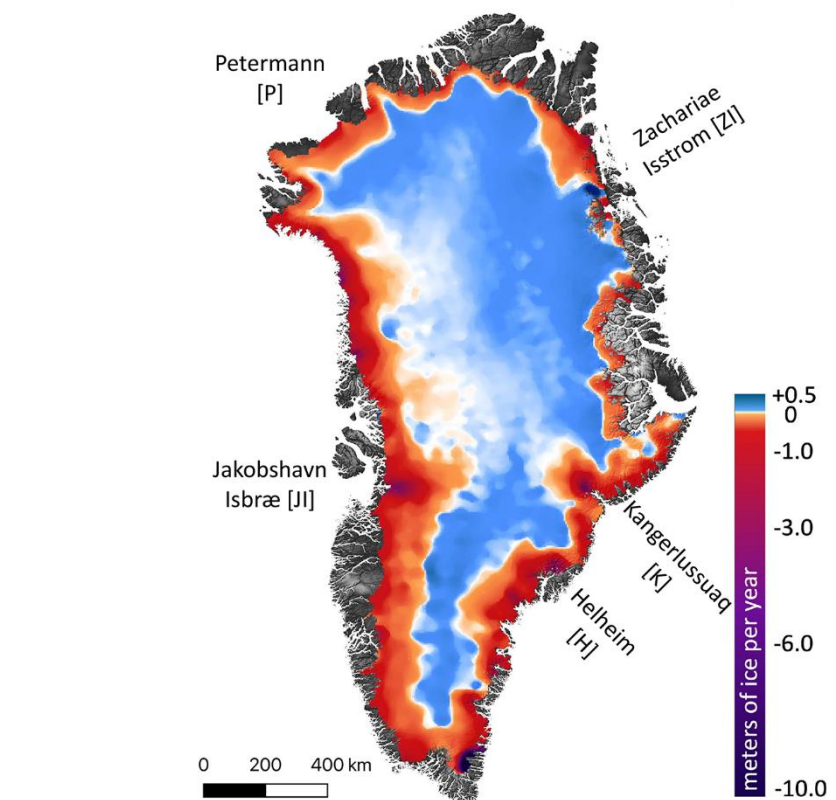


Fig. 2. Mass loss from Greenland Ice Sheet (2003–2019). (Top) Mass change (m ice equivalent per year). (Bottom) Mass changes around the margin. Map and ice margin mass change have been smoothed with a 35 km median filter for improved visualization.

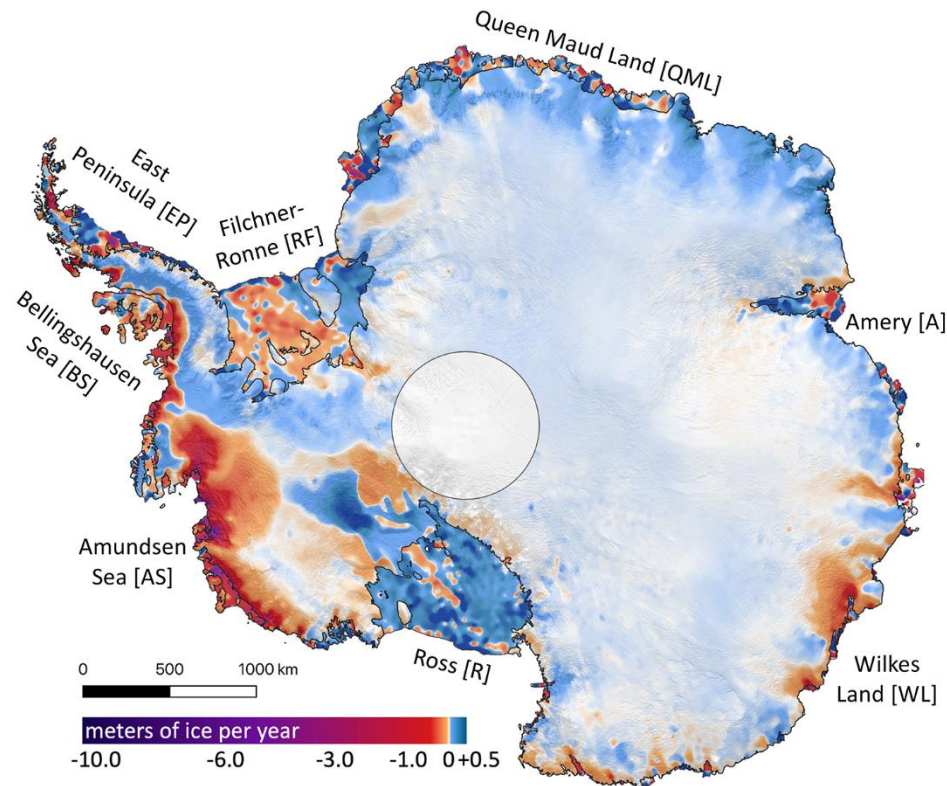


Fig. 3. Mass loss from Antarctica (2003–2019). (Top) Mass change for Antarctica. (Bottom) Mass changes at the grounding line. Highest mass loss rates are in West Antarctica and Wilkes Land, East Antarctica. Map and grounding line mass change have been smoothed with a 35 km median filter for improved visualization.

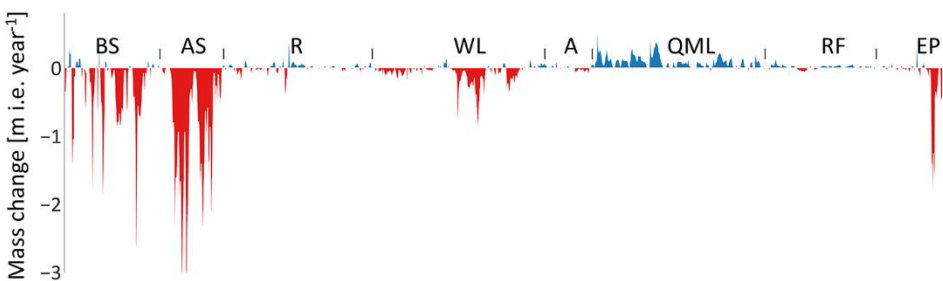


Table 1. Comparison of mass loss 2003–2019 for floating and grounded ice by region after (44): Greenland, East Antarctica (EAIS), West Antarctica (WAIS), the Antarctica Peninsula (AP) (see fig. S8). Cumulative ice loss/gain between 2003 and 2019 provided in Sea Level Equivalent units.

	dM/dt (Gt a⁻¹)		SLR potential (m)	Total SLE 2003–2019 (mm)
	Floating	Grounded		
Greenland	N/A	-200 ± 12	7.4	8.9
EAIS	106 ± 29	90 ± 21	51.1	-4.0
WAIS	-76 ± 49	-169 ± 10	5.6	7.5
AP	-14 ± 28	-39 ± 5	0.5	1.7
Antarctica	15 ± 65	-118 ± 24	57.2	5.2

Pervasive ice sheet mass loss reflects competing ocean and atmosphere processes

Ben Smith, Helen A. Fricker, Alex S. Gardner, Brooke Medley, Johan Nilsson, Fernando S. Paolo, Nicholas Holschuh, Susheel Adusumilli, Kelly Brunt, Bea Csatho, Kaitlin Harbeck, Thorsten Markus, Thomas Neumann, Matthew R. Siegfried and H. Jay Zwally

published online April 30, 2020

ARTICLE TOOLS

<http://science.scienmag.org/content/early/2020/04/29/science.aaz5845>

SUPPLEMENTARY MATERIALS

<http://science.scienmag.org/content/suppl/2020/04/29/science.aaz5845.DC1>

REFERENCES

This article cites 101 articles, 10 of which you can access for free

<http://science.scienmag.org/content/early/2020/04/29/science.aaz5845#BIBL>

PERMISSIONS

<http://www.scienmag.org/help/reprints-and-permissions>

Use of this article is subject to the [Terms of Service](#)

Science (print ISSN 0036-8075; online ISSN 1095-9203) is published by the American Association for the Advancement of Science, 1200 New York Avenue NW, Washington, DC 20005. The title *Science* is a registered trademark of AAAS.

Copyright © 2020, American Association for the Advancement of Science